EuroIntervention 2023;19:e383-e393 published online ahead of print June 2023 ■ published online e-edition August 2023

Mechanisms and treatment outcomes of ostial right coronary artery in-stent restenosis

Kei Yamamoto[1,2], MD; Takao Sato[1,2], MD; Hanan Salem[1,2,3], MD; Mitsuaki Matsumura[2], BS; Khady N. Fall[1], MD, MPH; Megha Prasad[1], MD, MS; Vivian G. Ng[1], MD; Sanjum S. Sethi[1], MD; Tamim M. Nazif[1,2], MD; Sahil A. Parikh[1,2], MD; Torsten P. Vahl[1,2], MD; Ziad A. Ali[2,4], MD, DPhil; Dimitri Karmpaliotis[2,5], MD, PhD; LeRoy E. Rabbani[1,2], MD; Michael B. Collins[1], MD; Martin B. Leon[1,2], MD; Margaret McEntegart[1,2], MD, PhD; Jeffery W. Moses[1,2], MD; Ajay J. Kirtane[1,2], MD, SM; Gary S. Mintz[2], MD; Akiko Maehara[1,2]*, MD

1. Division of Cardiology, Department of Medicine, Columbia University Medical Center, New York, NY, USA; 2. Clinical Trials Center, Cardiovascular Research Foundation, New York, NY, USA; 3. Cardiovascular Medicine Department, Faculty of Medicine - Tanta University, Tanta, Egypt; 4. St. Francis Hospital, Roslyn, NY, USA; 5. Gagnon Cardiovascular Institute, Morristown Medical Center, Morristown, NJ, USA

This paper also includes supplementary data published online at: https://eurointervention.pcronline.com/doi/10.4244/EIJ-D-23-00107

KEYWORDS

- in-stent restenosis
- intravascular ultrasound
- prior PCI

Abstract

Background: Despite a high rate of in-stent restenosis (ISR) after stenting the right coronary artery (RCA) ostium, the mechanism of ostial RCA ISR is not well understood.

Aims: We aimed to clarify the cause of ostial RCA ISR using intravascular ultrasound (IVUS).

Methods: Overall, 139 ostial RCA ISR lesions were identified with IVUS, pre-revascularisation. Primary ISR mechanisms were classified as follows: 1) neointimal hyperplasia (NIH); 2) neoatherosclerosis; 3) ostium not covered by the stent; 4) stent fracture or deformation; 5) stent underexpansion (old minimum stent area <4.0 mm^2 or stent expansion <50%); or 6) a protruding calcified nodule.

Results: The median duration from prior stenting was 1.2 (first quartile 0.6, third quartile 3.1) years. The primary mechanisms of ISR were NIH in 25% (n=35) of lesions, neoatherosclerosis in 22% (n=30), uncovered ostium in 6% (n=9) (biological cause 53%, n=74), stent fracture or deformation in 25% (n=35), underexpansion in 11% (n=15), and protruding calcified nodules in 11% (n=15) (mechanical cause 47%, n=65). Including secondary mechanisms, 51% (n=71) of ostial RCA ISRs had stent fractures that were associated with greater hinge motion of the ostial-aorta angle during the cardiac cycle. The Kaplan-Meier rate of target lesion failure at 1 year was 11.5%. When the mechanically caused ISRs were treated without new stents, they suffered a higher subsequent event rate (41.4%) compared with non-mechanical causes or mechanical causes treated without restenting (7.8%, unadjusted hazard ratio 6.44, 95% confidence interval: 2.33-17.78; p<0.0001).

Conclusions: Half of the ostial RCA ISRs were due to mechanical causes. Subsequent event rates were high, especially in mechanically caused ISRs treated without the implantation of a new stent.

**Corresponding author: Columbia University Medical Center, Cardiovascular Research Foundation, 1700 Broadway, 9th Floor, New York, NY 10019, USA. E-mail: amaehara@crf.org*

SUBMITTED ON 11/02/2023 - REVISION RECEIVED ON 1st 04/07/2023 / 2nd 26/04/2023 - ACCEPTED ON 28/04/2023

DOI: 10.4244/EIJ-D-23-00107

Abbreviations

CN	calcified nodule
DES	drug-eluting stent
ISR	in-stent restenosis
IVUS	intravascular ultrasound
MLA	minimum lumen area
MSA	minimum stent area
NIH	neointimal hyperplasia
PCI	percutaneous coronary intervention
RCA	right coronary artery

Introduction

Drug-eluting stents (DES) have dramatically decreased the incidence of in-stent restenosis (ISR)[1]. However, percutaneous coronary intervention (PCI) for an ostial right coronary artery (RCA) stenosis remains challenging. The prevalence of ostial RCA ISR has been reported as high as 7.5-12.7%[2,3], higher than the overall 2-year restenosis rate of 2.9-6.4% using contemporary DES[4,5]. The ostial RCA location is strongly associated with subsequent target vessel revascularisation[3]. Unique anatomical features of the ostial RCA, including poor distensibility and excessive hinge movement, have been reported along with a higher prevalence of stent fracture[6]. Despite this, a systematic morphological evaluation of ostial RCA ISR has not been done. The primary objective of the current study was to investigate the mechanism of ostial RCA ISR using intravascular ultrasound (IVUS). Additionally, we evaluated the association between the mechanism of ostial RCA ISR and subsequent long-term outcomes after repeat revascularisation.

Methods

STUDY DESIGN AND PATIENT POPULATION

This was a retrospective, observational, single-centre study at the New York-Presbyterian Hospital/Columbia University Medical Center (New York, NY, USA). ISR was defined as an angiographic visual estimation >50% diameter stenosis or IVUS minimum lumen area (MLA) <4 mm^2 [7]. An ostial RCA lesion was defined as a stenosis within 3 mm from the aorto-ostial junction[8]. Inclusion criteria were 1) patients who underwent repeat revascularisation due to ostial RCA ISR with clinical symptoms and 2) analysable IVUS images before any treatment or after predilation using a ≤2.5 mm balloon. ISR with multiple layers of stents were included. If a patient had undergone multiple repeat revascularisations related to an ostial RCA ISR lesion, only the first event was included.

Patient and procedural demographics were obtained from electronic medical records. Moderate or severe aortic stenosis was defined as an aortic valve area <1.5 cm^2 or a peak aortic velocity >3.0 m/sec[9]. This study was approved by the Institutional Review Board of Columbia University Medical Center which waived informed consent for the retrospective review of records as there was minimal risk.

ANGIOGRAPHIC ANALYSIS STRATEGY AND ASSESSMENT

Quantitative and qualitative angiographic analyses were performed by an experienced observer (T. Sato), blinded to clinical and IVUS findings, using QAngioXA (Medis Medical Imaging) and standardised methodology[8]. Only the distal reference was used to calculate the angiographic diameter stenosis. The angiographic pattern of ISR was classified as follows: 1) focal, ≤10 mm in length, which was further divided into stent edge (within 5 mm from the stent edge) or multifocal; 2) diffuse, >10 mm in length within the stent; 3) proliferative, >10 mm in length and extending beyond the stent edges; and 4) total occlusion.

Index coronary angiograms from the time of the original stent implantation procedure were also collected to assess the impact of the RCA hinge motion on ostial RCA ISR. The angles between the proximal segment of the RCA and the ascending aorta during systole and diastole were measured, and Δ angle was calculated[10] **(Supplementary Figure 1)**. Angles were measured 1) pre-stent implantation during the index procedure, 2) post-stent implantation during the index procedure, and 3) at the time of ISR identification.

IVUS ANALYSIS AND ASSESSMENT

IVUS was performed using a rotational catheter (40 MHz Atlantis or 40 or 60 MHz OPTICROSS [Boston Scientific Corporation]; 45 MHz Revolution or Refinity [Philips]; or 60 MHz Kodama HD [ACIST]) using motorised pullback at 0.5-1.0 mm/s. IVUS analysis was performed by consensus by 2 experienced readers (K. Yamamoto and A. Maehara) using planimetry software (echoPlaque 4.0 Analysis Software [INDEC Medical Systems]). Quantitative analysis included the cross-sectional area of the lumen, stent, and vessel at the MLA and minimum stent area (MSA) sites. The neointimal hyperplasia (NIH) area (stent area minus lumen area) and percentage NIH (NIH/stent area) were calculated. Stent expansion was defined as MSA divided by the largest reference lumen or stent area within 10 mm distal to the ostium[11]. Because these reference areas were larger than historical reference areas[12], we applied a stent expansion <50% as a criterion of underexpansion. Thus, stent underexpansion was defined as MSA <4 mm^2 or stent expansion <50%[7].

ENDPOINTS AND DEFINITIONS

The primary patterns of ISR were classified as 1) NIH **(Figure 1A)**, 2) neoatherosclesrosis **(Figure 1B)**, 3) uncovered ostial lesion **(Figure 1C)**, 4) stent fracture or deformation **(Figure 1D)**, 5) stent underexpansion **(Figure 1E)**, or 6) a protruding calcified nodule (CN) **(Figure 1F)**. The primary clinical outcome was target lesion failure (TLF): a composite of cardiac death, target vessel myocardial infarction (MI), or clinically driven target lesion revascularisation (TLR).

Neoatherosclerosis was defined as atherosclerotic changes at the MLA site within the stent. It was either calcified NIH (hyperechoic tissue with acoustic shadowing), attenuated NIH (ultrasound shadowing despite the absence of superficial calcium), or ruptured NIH (a cavity within NIH)[13]. When a calcified nodule was within the neoatherosclerotic calcified NIH, it was categorised as a neoatherosclerotic calcified nodule **(Supplementary Figure 2)**.

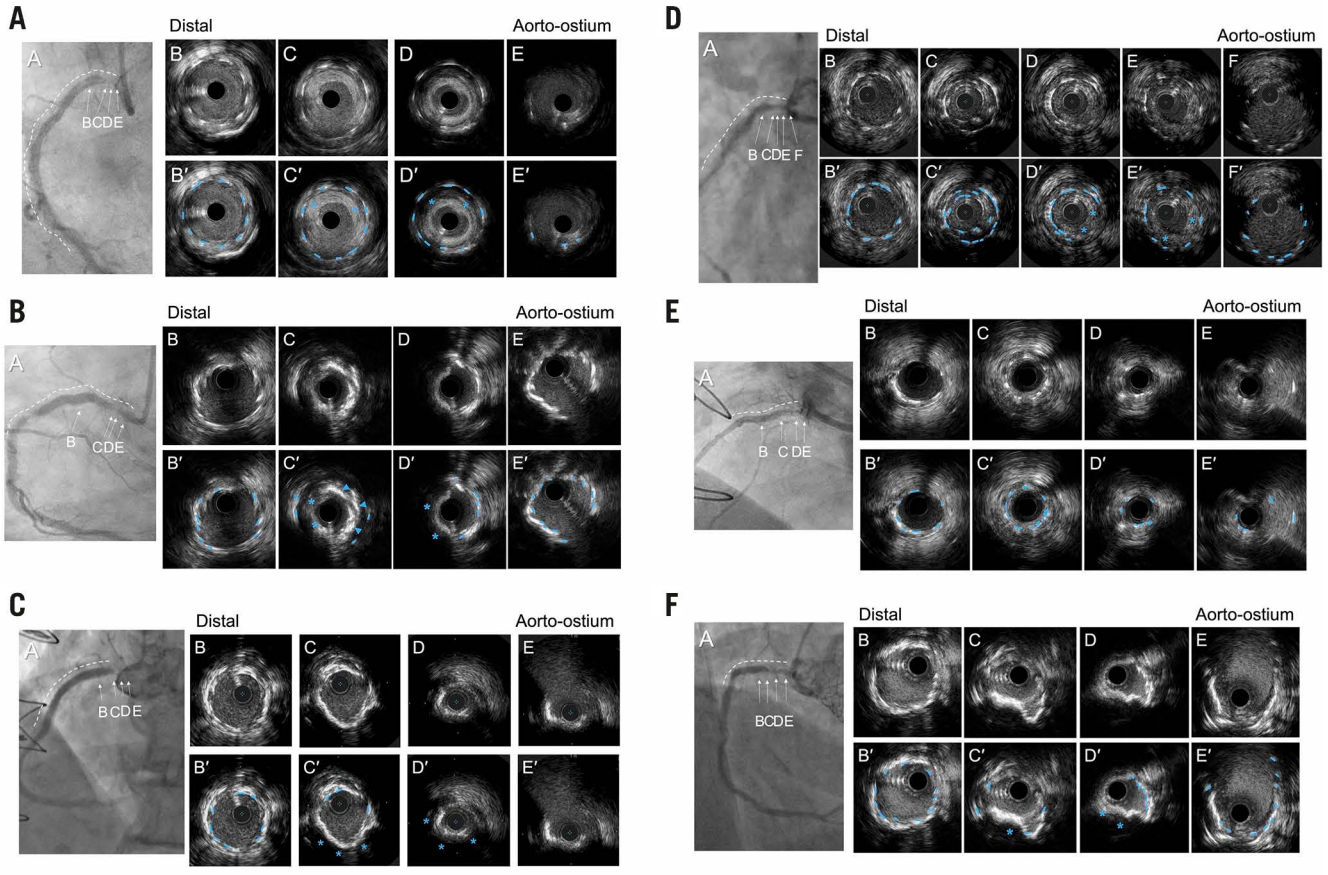

Figure 1. *Representative cases for each pattern. In each example, the coronary angiogram at the time of ISR (A) is shown accompanied by a white dotted line indicating the old stents. B-E in the coronary angiograms correspond to the IVUS image (B-E). B′-E′ are the same images with annotation compared with B-E. Blue dotted lines in the IVUS images indicate old stent struts. A) Excessive neointimal hyperplasia with good stent expansion; the blue asterisks indicate excessive neointimal hyperplasia. B) Neoatherosclerosis with good stent expansion; the blue arrowheads indicate neointimal calcium (superficial hyperintensity with acoustic shadow), and the blue asterisks indicate neointimal attenuated plaque (signal attenuation without calcium) representing lipidic plaque. These represent neoatherosclerosis within the old stent. C) Ostial restenosis without coverage of the ostium; the stent struts (blue dotted lines) were observed only in B and C with no struts in D and E indicating the lack of ostial stent coverage associated with a new stenosis. D) Overlap type stent fracture. Within a single-stent segment, 2 layers of old stent struts were observed (blue dotted lines) along with neointimal hyperplasia (blue asterisks). The inner stent layer measured 4.6 mm^2 in C, smaller than the distal non-fractured stent area (8.9 mm^2) in B. E) Underexpanded stent with minimal neointimal hyperplasia. A severely underexpanded stent (minimum stent area =2.2 mm^2) at D compared to the distal segment (stent area of 5.2 mm^2) in B. Neointimal hyperplasia at D measured 43%. F) Protruding calcified nodule within the stent. A calcified nodule (blue asterisks) was observed within the old stent struts (blue dotted lines) without adjacent neointimal hyperplasia. ISR: in-stent restenosis; IVUS: intravascular ultrasound*

A non-neoatherosclerotic protruding calcified nodule was an irregular convex-shaped calcium deposit within the old stent without adjacent NIH[14], which was not considered neoatherosclerosis.

Stent fracture included a double layer of struts within a single stent with preserved three-dimensional (3D) stent integrity, usually located in the middle of the stent, assuming that the stent struts were overlapped after the fracture (overlap type), or the dislocated or separated struts of a single stent (non-overlap type). Stent deformation was defined as multiple layers of struts seen within a single stent with a loss of 3D stent integrity, usually located at the proximal stent edge[15] **(Supplementary Figure 3)**.

An uncovered ostial lesion was defined as an unstented aorto-ostial stenosis proximal to an implanted stent. Aorto-ostial stent coverage was further categorised as full (360º of visible struts at the ostium), partial (<360º of visible stent struts at the ostium), or no coverage (no visible stent struts at the ostium). If the stent protruded into the aorta >1 mm, it was defined as a protruding stent **(Supplementary Figure 4)**.

The core lab assessment of the underlying mechanisms is shown in **Figure 2**. If there were multiple potential causes, the primary cause of ISR was diagnosed based on its greatest impact on stenosis. If there was either a non-neoatherosclerotic protruding calcified nodule within the stent or an uncovered aorto-ostial stenosis, that "mechanism" was considered to be the primary cause of ISR. Typically, a non-neoatherosclerotic protruding calcified nodule does not accompany stent underexpansion and NIH. When there

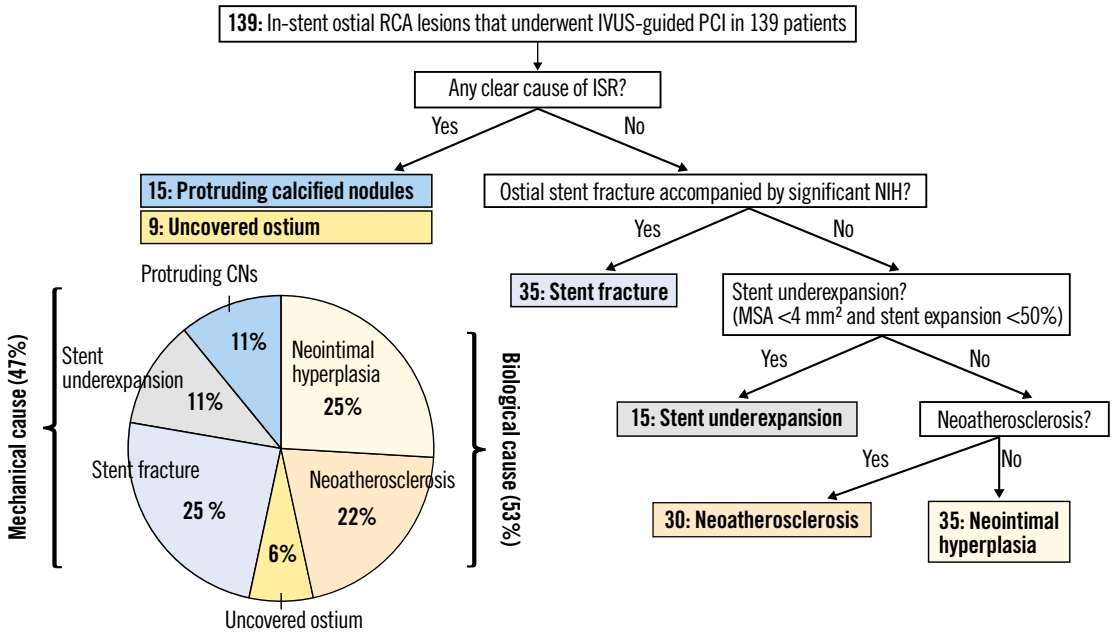

Figure 2. *Diagnostic flowchart of each primary cause. For ISRs with multiple patterns, the primary pattern was hierarchally diagnosed based on the main morphology at the stenosis. The prevalence of biological causes (neointimal hyperplasia, neoatherosclerosis, or uncovered ostium) was 53% and 47% for mechanical causes. CN: calcified nodules; ISR: in-stent restenosis; IVUS: intravascular ultrasound; MSA: minimum stent area; NIH: neointimal hyperplasia; RCA: right coronary artery; PCI: percutaneous coronary intervention*

was an uncovered aorto-ostial stenosis, symptoms remained and the patients came back early. The MLA was located at the uncovered ostial stenosis proximal to the stent which had only limited NIH. If there was an ostial stent fracture along with focal NIH without other causes, stent fracture was considered to be the primary cause of ISR. If there was a stent underexpansion with limited NIH, stent underexpansion was considered to be the primary cause of ISR. The rest of the ISRs, those with only tissue proliferation and no other mechanism of ISR (e.g., no calcified nodule, no stent underexpansion, no stent fracture, etc.) were further divided into neoatherosclerosis versus NIH.

STATISTICAL ANALYSIS

Categorical variables were presented as counts and percentages and compared with the χ^2 or Fisher's exact test, as appropriate. Normally distributed continuous variables were presented as mean and standard deviation and compared with the Student's t-test and non-normally distributed continuous variables were presented as median (first quartile, third quartile) and compared with the Mann-Whitney U test. Inter- and intraobserver variability was tested using intraclass correlation coefficient for Δ ostial-aorta angle using 40 randomly selected cases. Interobserver variability was assessed by 2 independent observers (T. Sato and K. Yamamoto), and intraobserver variability was assessed with reanalysis by a single observer 4 weeks later. The cumulative rate of TLF was estimated from Kaplan-Meier curves and compared using the log-rank test. A 2-sided $p<0.05$ was considered statistically significant. The association between the new stent implantation (dependent variable) and the presence of multiple layers of stent (independent variable) was tested using logistic regression models. Analysis was performed using R software version 4.0.3 (R Foundation for Statistical Computing).

Results

Between January 2005 and September 2020, IVUS was performed in 5,102 RCA lesions, including 216 ostial RCA ISR lesions, from which we identified 139 lesions meeting the inclusion criteria **(Supplementary Figure 5)**. Predilation with a ≤2.5 mm balloon was required in 29% (n=41) of lesions. Clinical characteristics have been summarised in **Table 1**. The median (first quartile [Q1], third quartile [Q3]) duration from prior stent implantation was 1.2 (Q1 0.6, Q3 3.1) years. Index procedure information was available in 105 patients, and 69.5% of the older stents were second-generation DES **(Supplementary Table 1)**. The median patient age was 71 years, 42.4% were women, and 10.1% had prior or current moderate to severe aortic stenosis. Angiographic and procedural findings have been summarised in **Table 2**. Most ISR patterns (86.3%) were focal.

PRIMARY MECHANISM OF OSTIAL RCA ISR

The primary causes of ISR were neointimal hyperplasia in 25% (n=35) of lesions, neoatherosclerosis in 22% (n=30), uncovered ostium in 6% (n=9), stent fracture or deformation in 25% (n=35), stent underexpansion in 11% (n=15), and protruding calcified nodule in 11% (n=15). A biological cause, including NIH, neoatherosclerosis, and uncovered ostium, was seen in 53%; and a mechanical cause (stent fracture or deformation, stent underexpansion, and protruding calcified nodule) was seen in 47% **(Figure 2)**. When we considered secondary causes of ISR, there were 43 lesions with

Table 1. Clinical characteristics and symptoms at the time of in-stent restenosis.

	n=139
Age, years	71 (66, 78)
Women	59 (42.4)
Hypertension	137 (98.5)
Dyslipidaemia	139 (100)
Diabetes mellitus	73 (52.5)
Insulin-treated	21 (15.1)
Chronic kidney disease*	58 (41.7)
Dialysis	6 (4.3)
Peripheral artery disease	34 (24.5)
Prior myocardial infarction	35 (25.1)
Prior coronary artery bypass grafting	27 (19.4)
Prior or current moderate or severe aortic stenosis	14 (10.1)
Duration from prior stent implantation, years	1.2 (0.6, 3.1)
Clinical presentation at the time of ISR	
Non-ST-elevation myocardial infarction	16 (11.5)
Unstable angina	65 (46.8)
Stable coronary artery disease	57 (41.0)

Values are n (%) or median (first quartile, third quartile). *Defined as estimated glomerular filtration rate <60 mL/min/1.73 m^2, calculated using the Modification of Diet in Renal Disease equation. ISR: in-stent restenosis

Table 2. Procedural and angiographic findings.

		n=139
Multivessel disease*		111 (79.9)
Calcification of ascending aorta		42 (30.2)
Target lesion calcification	Moderate	43 (30.9)
	Severe	34 (24.5)
	Radiolucent mass	14 (10.1)
In-stent restenosis pattern	Focal	120 (86.3)
	Proximal stent edge	100 (71.9)
	Multifocal	20 (14.4)
	Diffuse	8 (5.8)
	Proliferative	1 (0.7)
	Total occlusion	10 (7.2)
Quantitative coronary angiography	Lesion length, mm	7.0 (5.2, 11.7)
	Reference vessel diameter, mm	2.8 (2.5, 3.1)
Minimum lumen diameter, mm	Pre-PCI	1.1 (0.76, 1.4)
	Post-PCI	2.7 (2.4, 3.0)
Diameter stenosis, %	Pre-PCI	62.6 (49.8, 71.5)
	Post-PCI	13.2 (7.9, 21.0)
New stent implantation		93 (66.9)
Total new stent length, mm		22 (15, 41.5)
Plain balloon angioplasty only		46 (33.1)

Values are n (%) or median (first quartile, third quartile). *Defined as the presence of >50% diameter stenosis in 2 or more major epicardial arteries. PCI: percutaneous coronary intervention

more than one possible mechanism. If we included only the ISRs without predilation, the prevalence of a mechanical cause (48%) was consistent with the overall rate **(Supplementary Table 2)**. Among 35 ISRs with a primary cause of stent fracture or deformation, there were 24 fractures with overlapping stent struts, 2 without overlapping stent struts, and 9 deformations. As shown in **Supplementary Figure 3**, the stent area of inner layer of overlapped or deformed stent struts was smaller than the stent area at the adjacent non-fracture site. Focal NIHs were only found at the site of a fracture or deformation. Of note, there were no ISRs with primary stent underexpansion and neoatherosclerosis.

IVUS findings have been summarised in **Table 3**. The maximum calcium arc within the stent measured 90 (0, 152)°, and the maximum calcium arc behind the stent measured 187 (108, 304)°. The maximum calcium arc behind the stent was larger in cases with a protruding calcified nodule (242 [157, 360]°), stent underexpansion (225 [170, 360]°), or stent fracture (192 [72, 269]°), compared with other causes of ISR (NIH; 68 [0, 118]°, neoatherosclerosis 127 [67, 246]°, or uncovered ostium 99 [24, 165]°).

The relationship between the median duration since the index PCI and the mechanisms of ostial RCA ISR has been summarised in **Supplementary Figure 6**. The duration from stent implantation to ISR was the shortest for an uncovered ostium (0.5 [0.2, 0.6] years), followed by a protruding calcified nodule (0.7 [0.5, 1.8] years), NIH (1.5 [0.6, 3.2] years), stent fracture (1.8 [0.7, 3.9] years), stent underexpansion (2.7 [0.4, 3.6] years), and finally, neoatherosclerosis, which was the longest (2.7 [1.0, 5.0] years).

STENT FRACTURE/DEFORMATION

When secondary causes were included, 51% (71/139) of ostial RCA ISRs had evidence of stent fracture or deformation. The patterns of stent fracture were overlapping stent struts within a single stent in 52% (37/71), non-overlapping fracture in 34% (24/71), and deformation in 14% (10/71), with no difference in the angiographical characteristics between ISR with versus without stent fracture **(Supplementary Table 3)**.

A total of 59 index coronary angiograms from the original stent implantation procedure were available, and we compared 27 lesions with fracture at follow-up versus 32 lesions without fracture at follow-up **(Supplementary Figure 7, Table 4)**. A second-generation DES was implanted in 79.7% of lesions, and the median duration from prior stenting was 1.2 years without any difference based on the presence of stent fracture at follow-up. At the index procedure, the pre-PCI Δ ostial-aorta angle during the cardiac cycle was significantly greater in lesions with fracture versus those without fracture (21 [12, 27] ° vs 10 [7,17] °; p=0.003). The change in Δ ostial-aorta angle from pre- to post-procedure was also significantly greater in lesions with fracture versus those without fracture (7 [–0.5, 13] ° vs 0.1 [–3, 5] °; p=0.01). There was a good inter-/intraobserver agreement for Δ ostial-aorta angle (hinge motion assessment). The intraclass correlation coefficients for interobserver and intraobserver agreement of measurements for Δ ostial-aorta angle were 0.85 and 0.83, respectively.

Table 3. Intravascular ultrasound findings.

	n=139
Preprocedure	
Minimum lumen area, mm²	2.6 (2.1, 3.0)
Minimum stent area, mm²	6.4 (4.9, 7.4)
Minimum stent area <4.0 mm²	20 (14.4)
Minimum stent expansion, %	68.8 (56.9, 79.4)
Minimum stent expansion <70%	75 (53.9)
Minimum stent expansion <50%	20 (14.4)
MSA <4.0 mm² or stent expansion <50%	30 (21.6)
Largest stent area, mm²	9.5 (7.9, 10.5)
Stent eccentricity index	0.80 (0.76, 0.83)
Maximum neointimal hyperplasia area, %	58.9 (50.9, 68.3)
Maximum calcium arc behind the stent, °	187 (108, 304)
Maximum calcium arc within the stent,°	90 (0, 152)
Any stent fracture	71 (51.1)
Overlap	49 (35.2)
No overlap	10 (7.2)
Deformation	12 (8.6)
Old stent RCA ostial coverage in 112 ostial evaluable lesions	
Full coverage	57 (50.9)
Protruding >1 mm	13 (11.6)
Not protruding	44 (39.3)
Partial coverage	22 (19.6)
No coverage	33 (29.5)
Wire entering from lateral stent strut	8 (5.8)
Post-procedure	
Minimum stent area*, mm²	6.8 (5.7, 7.8)
Minimum stent expansion, %	70.5 (60.0, 79.3)
Stent eccentricity index	0.80 (0.75, 0.85)

Values are n (%) or median (first quartile, third quartile). *New stent area (if new stent was implanted), otherwise, old stent area post-ballooning. MSA: minimum stent area; RCA: right coronary artery

All lesions were treated successfully, and a new stent was deployed in 66.9% of patients. The rate of restenting was lower in mechanically caused ISRs (49.3%, 32/65) compared with biologically caused ISRs (82.4%, 61/74; p<0.001) **(Figure 3)**. Of note, during the study duration, drug-coated balloons were not available in the US. Operators were reluctant to deploy additional new stents when multiple layers of old stents were found (odds ratio 0.26 [0.11, 0.59]; p=0.001). Postprocedural MSA and stent expansion were 6.8 (5.5, 7.8) mm² and 70.5 (60.0, 79.3) %, respectively.

CLINICAL OUTCOMES

The median follow-up duration after repeat revascularisation was 1.8 (0.2, 3.8) years. The overall Kaplan-Meier rate of TLF at 1 year was 11.5%, including 15 clinically driven target lesion revascularisations and 1 cardiac death. We divided the ISRs into 4 groups: 32 ISRs with a mechanical cause with new stent implantation, 33 ISRs with a mechanical cause without a new stent, 61 ISRs with a biological cause with a new stent, and 13 ISRs with a biological cause without a new stent. Among the 65 ISRs with a mechanical cause, the postprocedural minimum lumen diameter was smaller in the ISRs without new stents, the median 2.3 (2.2, 2.6) mm compared with the ISRs treated with a new stent, 2.7 (2.4, 3.0) mm; p=0.01. **(Supplementary Table 4)**. Mechanical causes that were not treated with a new stent had a higher subsequent TLF rate (41.4%) compared with the other 3 groups (7.8%, unadjusted hazard ratio 6.44, 95% confidence interval: 2.33-17.78; p<0.0001)

Discussion

The key findings of the present study were as follows: 1) approximately half of ostial RCA ISRs had a mechanical cause, including stent fracture, stent underexpansion, or protruding calcium; 2) stent fractures appeared in 51% of ostial RCA ISRs and were associated with greater motion at the RCA ostial hinge point; 3) subsequent event rates were high, especially in the mechanically caused ISRs without a new stent implantation **(Central illustration)**.

HIGHER PREVALENCE OF RESTENOSIS AT THE OSTIAL RCA LOCATION

The ostial RCA has the following histological characteristics: 1) fibrotic and sclerotic plaque that contains smooth muscle, collagen tissue, and calcification; 2) muscle bundle that independently arises from the elastin muscle fibre of the aorta; and 3) thick adventitia[16].

In the balloon angioplasty era, coronary angioplasty for ostial RCA had a poor success rate (88%) with a high rate of acute complications, including acute occlusion (8%) and repeat revascularisation (47%), suggesting greater elastic recoil compared with non-RCA ostial lesions[17].

Bare metal stents improved the success rate (96%) and decreased the rate of repeat revascularisation (24%)[17]. DES further decreased the rate of repeat revascularisation compared to bare metal stents. However, outcomes of ostial RCA are still not acceptable, even with newer DES[3].

Forty-seven percent of the ISRs showed tissue proliferation within the stent (NIH or neoatherosclerosis). Neoatherosclerosis was observed later than NIH. This corresponds to the results of optical coherence tomography (OCT) ISR reports, which revealed neoatherosclerosis in 25% of any ISR and 29% of ISR implanted for >1 year[7].

STENT FRACTURE AND CHRONIC RECOIL

Stent fractures were found in 51% of ostial RCA ISRs, much higher than previous "all lesions" reports, which reported 9.6% by IVUS[15], 12.7% by OCT[18], and 29% by pathology[19]. Angiographically, stent fractures have been associated with RCA lesions[6], and an RCA hinge motion and ostial location have been predictors of stent fracture, as was also seen in the current study[10]. Moreover, the morphological characteristics of the ostial RCA including poor arterial distensibility and excessive rigidity[20] could contribute to stent recoil and fracture. Tsunoda et al revealed that the stent area at the RCA ostium in 19 patients measured 8.1±1.5 mm² after

Table 4. Comparison of vessel bending between lesions with versus without stent fracture as a cause of ostial RCA ISR.

Variable	All (n=59)	Lesions with fracture (n=27)	Lesions without fracture (n = 32)	*p*-value
Stent type during index procedure				
Bare metal stent	1 (1.7)	0 (0.0)	1 (3.1)	0.86
1st-generation drug-eluting stent	11 (18.6)	6 (22.2)	5 (15.6)	
2nd-generation drug-eluting stent	47 (79.7)	21 (77.8)	26 (81.3)	
Duration from prior stenting, years	1.2 (0.6, 3.2)	1.1 (0.7, 2.9)	1.2 (0.6, 3.2)	0.85
At index				
Pre-PCI				
Maximum ostial-aorta angle, °	73 (60, 91)	83 (62, 96)	72 (52, 90)	0.18
Minimum ostial-aorta angle, °	58 (41, 77)	58 (41, 74)	59 (39, 80)	0.99
Δ ostial-aorta angle, °	14 (7, 21)	21 (12, 27)	10 (7, 17)	0.003
Post-PCI				
Maximum ostial-aorta angle, °	73 (61, 89)	79 (64, 91)	70 (52, 85)	0.08
Minimum ostial-aorta angle, °	62 (45, 75)	65 (52, 77)	57 (43, 72)	0.10
Δ ostial-aorta angle, °	11 (6, 18)	13 (7, 19)	10 (5, 19)	0.052
Pre- to post- change of Δ ostial-aorta angle, °	3 (–2, 8)	7 (–0.5, 13)	0.1 (–3, 5)	0.01
At event				
Pre-revascularisation				
Maximum ostial-aorta angle, °	73 (57, 87)	73 (57, 81)	74 (59, 86)	0.58
Minimum ostial-aorta angle, °	61 (47, 77)	59 (45, 74)	63 (49, 78)	0.30
Δ ostial-aorta angle, °	10 (7, 14)	11 (8, 20)	11 (7, 15)	0.62
Index to event change of Δ ostial-aorta angle	0.7 (–3, 4)	0.1 (–6, 3)	1 (–3, 4)	0.73

Values are n (%) or median (first quartile, third quartile). ISR: in-stent restenosis; PCI: percutaneous coronary intervention; RCA: right coronary artery

stenting and 6.4±1.9 mm^2 at follow-up, indicating chronic stent recoil[21]. One case in the present study also showed that the stent area changed from 6.4 mm^2 to 5.4 mm^2 **(Supplementary Figure 8)**.

PROTRUDING CALCIFIED NODULE WITHIN THE STENT

Pathologically, calcified nodules are associated with breaks in the calcified sheets caused by motion stress, as was seen in the current study[22]. Nakamura et al suggested that one potential mechanism of ostial RCA ISR was the protrusion of a calcified nodule through the struts at the time of stenting[14]. Sugane et al reported that stenting a culprit calcified nodule in patients with an acute coronary syndrome was associated with a recurrence of the calcified nodule within the stent in more than 80%[23] of patients. The present study also revealed that protruding calcified nodules were seen in the early phase (median 0.7 years) from stent implantation. As neoatherosclerosis was seen in the late phase, the duration can help to distinguish protruding calcified nodules from calcified neoatherosclerosis, as well as the presence of adjacent calcium **(Supplementary Figure 2)**.

MISSING STENT IMPLANTATION

Optimal positioning of an ostial stent can be difficult. Residual stenosis at a stent edge is a known risk for future revascularisation[24]. Dishmon et al reported that 54% of ostial stents had geographical miss[25]. In the 3D analysis from computed tomography (CT), only 13% of procedures resulted in complete ostial coverage, whereas 95% were considered as having optimal coverage by the coronary angiogram[26]. Approximately half showed a partially or completely uncovered ostium in the current study, when taking into account both the primary and secondary mechanisms.

CLINICAL IMPLICATIONS

There are 3 general clinical implications of this study. First, there are clear lessons to be learned to avoid RCA ISR when implanting a DES: making sure that the ostium is covered and optimising stent expansion, ideally using IVUS guidance[27]. Second, the frequent finding of stent fracture suggests that interventional cardiologists should consider a more robust stent when treating an RCA aorto-ostial lesion[11]. Finally, correcting the underlying mechanisms may improve long-term outcomes. For example, if there is an underexpansion due to severe calcium, intravascular lithotripsy should be considered at the time of ISR[28]. If stent fracture/deformation or chronic recoil is found at the time of ISR, an additional stronger stent should be considered[29]. Drug-coated balloons should be considered in cases with multiple stent layers[30].

Study limitations

There are several limitations in the present study. First, this was a retrospective, observational study of patients with analysable

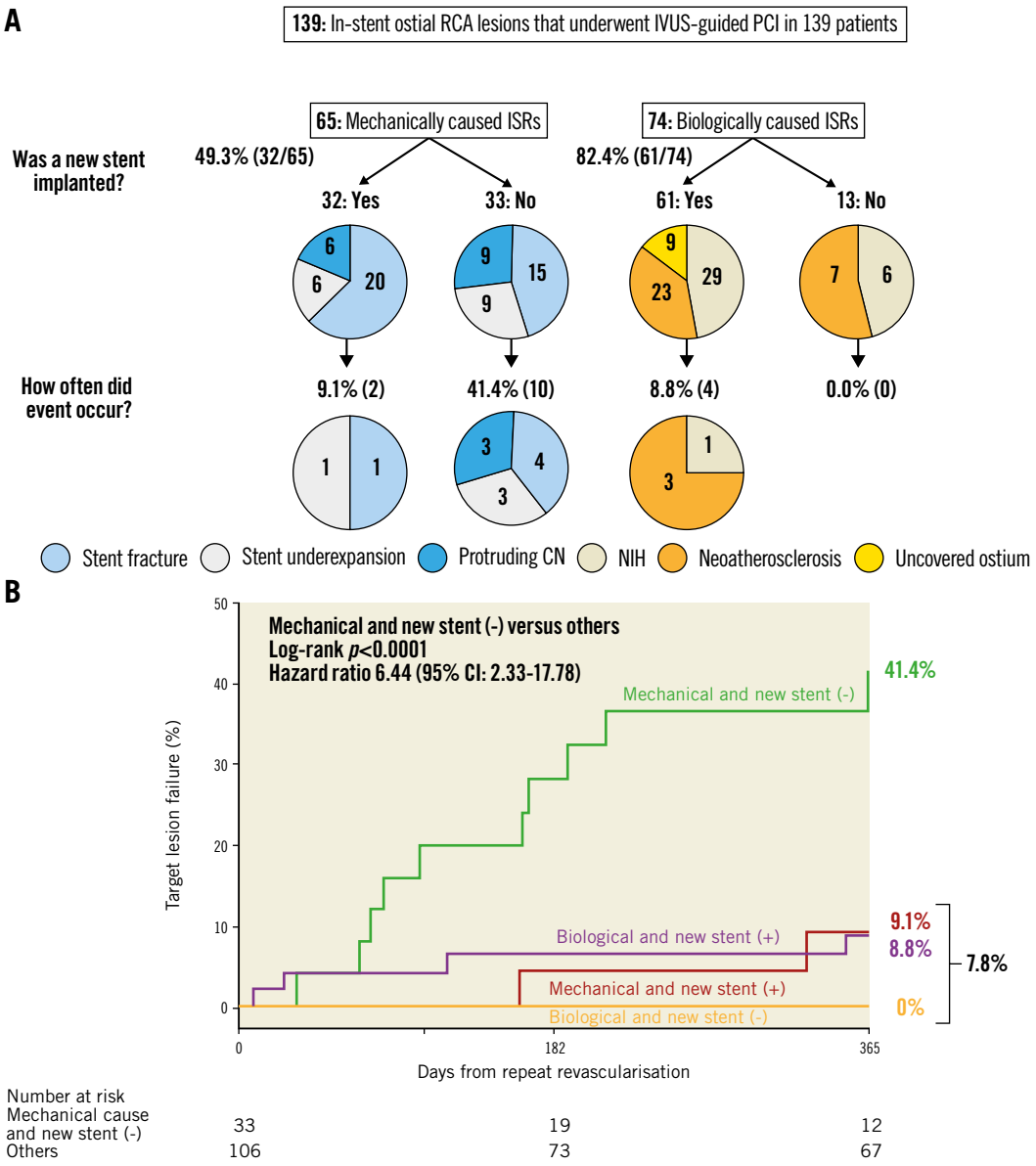

Figure 3. *Clinical outcomes of mechanical and biological causes with or without new stents. A) The prevalence of each primary cause with or without new stent implantation. B) Kaplan-Meier curves for target lesion failure due to a mechanical cause without a new stent vs others. CI: confidence interval; CN: calcified nodules; ISR: in-stent restenosis; IVUS: intravascular ultrasound; MSA: minimum stent area; NIH: neointimal hyperplasia; RCA: right coronary artery; PCI: percutaneous coronary intervention*

pre-intervention IVUS. Out of 216 procedures, the final enrolment included only 139 cases (64.4%). Thus, there was a selection bias; therefore, cautious interpretation is necessary. Second, we did not have enough index IVUS images to evaluate chronic stent recoil. Third, IVUS had limitations regarding restenostic tissue characterisation and tracing of stent struts. In some cases, differentiation among protruding calcified nodules, neoatherosclerotic calcified nodules, or calcified nodules behind the stent was difficult **(Supplementary Figure 2)**. Fourth, we included cases with predilatation (29.5% of cases) that may have affected ISR morphology. However, a sensitivity analysis, only including cases without predilation, showed a consistent result **(Supplementary Table 1)**. Fifth, because there were multifactorial causes, the classification of the primary cause could be misunderstood. Sixth, only 59 index angiograms at the stent implantation were available, which might have lead to selection bias in analysing stent fractures and angle relationship. Finally, even if the underlying morphology is recognised, some factors such as hinge motion can only be minimally modified.

Conclusions

Half of the analysed ostial RCA ISRs were due to mechanical causes, including stent fracture, stent underexpansion, and protruding calcified nodules. Subsequent event rates were high, especially in the mechanically caused ISRs that did not receive a new stent implantation.

EuroIntervention

CENTRAL **ILLUSTRATION** Ostial RCA ISR: mechanisms and outcomes.

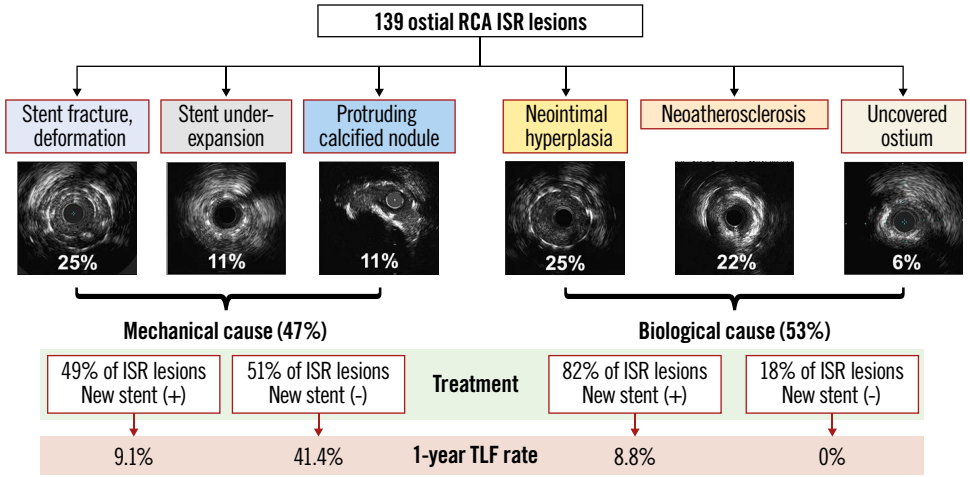

ISR: in-stent restenosis; RCA: right coronary artery; TLF: target lesion failure

Impact on daily practice

Mechanically caused ostial RCA ISRs should have the specific cause addressed at the time of ISR presentation. Including secondary mechanisms, 51% of ostial RCA ISRs had evidence of stent fracture and a greater change in the ostial-aorta angle during the cardiac cycle (hinge motion), which was associated with stent fracture. The current analysis suggests potential ways to reduce the rate of ostial RCA ISR, including appropriate stent positioning, modification of calcified nodules, and use of stronger stents that are better suited to resist fracture and deformation.

Conflict of interest statement

M. Matsumura is a consultant for Terumo Corp, and Boston Scientific. K.N. Fall is a consultant for Infraredx and Boston Scientific. M. Prasad is a consultant for Abbott Vascular; and is on the speaker`s bureau of Philips and Neovasc. S.A. Parikh has done research for Abbott, Boston Scientific, Surmodics, TriReme, Shockwave, and Veryan Medical; is on the advisory boards of Abbott, Boston Scientific, Cordis, Medtronic, CSI, and Philips; and has been a consultant for Inari, Penumbra, Terumo, and Abiomed. Z.A. Ali has received grants from Abbott Vascular and CSI; is a consultant for Amgen, AstraZeneca, and Boston Scientific; and has equity in Shockwave. D. Karmpaliotis has received honoraria from Boston Scientific and Abbott Vascular; and has equity in Saranas Soundbite and Traverse Vascular. M.B. Leon has received institutional clinical research grants from Abbott Vascular, Boston Scientific, and Medtronic. M. McEntegart has received honoraria from Boston Scientific, Abbott Vascular, Shockwave Medical, Teleflex, and Biosensors. A.J. Kirtan has received institutional funding for Columbia University and/or the Cardiovascular Research Foundation from Medtronic, Boston Scientific, Abbott Vascular, Abiomed, CSI, Siemens, Philips, ReCor Medical, and Neurotronic (institutional funding includes fees paid to Columbia University and/or Cardiovascular Research Foundation for consulting and/or speaking engagements in which he controlled the content); has been a consultant for IMDS; and has received travel expenses/meals from Medtronic, Boston Scientific, Abbott Vascular, Abiomed, CSI, Siemens, Philips, ReCor Medical, Chiesi, OpSens, Zoll, and Regeneron. G.S. Mintz has received honoraria from Boston Scientific, Philips, Abiomed, and Medtronic. A. Maehara has received research grants from Boston Scientific and Abbott Vascular; and is a consultant for Boston Scientific and Philips. The other authors have no conflicts of interest to declare.

References

1. Piccolo R, Bonaa KH, Efthimiou O, Varenne O, Baldo A, Urban P, Kaiser C, Remkes W, Raber L, de Belder A, van 't Hof AWJ, Stankovic G, Lemos PA, Wilsgaard T, Reifart J, Rodriguez AE, Ribeiro EE, Serruys PWJC, Abizaid A, Sabaté M, Byrne RA, de la Torre Hernandez JM, Wijns W, Jüni P, Windecker S, Valgimigli M; Coronary Stent Trialists' Collaboration. Drug-eluting or bare-metal stents for percutaneous coronary intervention: a systematic review and individual patient data meta-analysis of randomised clinical trials. *Lancet.* 2019;393:2503-10.

2. Watanabe Y, Takagi K, Naganuma T, Nakamura S. Comparison of early- and new-generation drug-eluting stent implantations for ostial right coronary artery lesions. *Cardiovasc Ther.* 2017;35.

3. Lam MK, Sen H, Tandjung K, Lowik MM, Basalus MW, Mewes JC, Stoel MG, van Houwelingen KG, Linssen GC, Ijzerman MJ, Doggen CJ, von Birgelen C. Clinical outcome of patients with implantation of second-generation drug-eluting stents in the right coronary ostium: insights from 2-year follow-up of the TWENTE trial. *Catheter Cardiovasc Interv.* 2015;85:524-31.

4. Zbinden R, Piccolo R, Heg D, Roffi M, Kurz DJ, Muller O, Vuilliomenet A, Cook S, Weilenmann D, Kaiser C, Jamshidi P, Franzone A, Eberli F, Jüni P, Windecker S, Pilgrim T. Ultrathin Strut Biodegradable Polymer Sirolimus-Eluting Stent Versus Durable-Polymer Everolimus-Eluting Stent for Percutaneous Coronary Revascularization: 2-Year Results of the BIOSCIENCE Trial. *J Am Heart Assoc.* 2016;5:e003255.

5. Tandjung K, Sen H, Lam MK, Basalus MWZ, Louwerenburg JHW, Stoel MG, van Houwelingen KG, de Man FHAF, Linssen GCM, Said SAM, Nienhuis MB, Löwik MM, Verhorst PMJ, van der Palen J, von Birgelen C. Clinical outcome following stringent discontinuation of dual antiplatelet therapy after 12 months in real-world patients treated with second-generation zotarolimus-eluting resolute and everolimus-eluting Xience V stents: 2-year follow-up of the randomized TWENTE trial. *J Am Coll Cardiol.* 2013;61:2406-16.

6. Kan J, Ge Z, Zhang JJ, Liu ZZ, Tian NL, Ye F, Li SJ, Qian XS, Yang S, Chen MX, Rab T, Chen SL. Incidence and Clinical Outcomes of Stent Fractures on the Basis of 6,555 Patients and 16,482 Drug-Eluting Stents From 4 Centers. *JACC Cardiovasc Interv.* 2016;9:1115-23.

7. Song L, Mintz GS, Yin D, Yamamoto MH, Chin CY, Matsumura M, Kirtane AJ, Parikh MA, Moses JW, Ali ZA, Shlofmitz RA, Maehara A. Characteristics of early versus late in-stent restenosis in second-generation drug-eluting stents: an optical coherence tomography study. *EuroIntervention.* 2017;13:294-302.

8. Andalib A, Almonacid A, Popma J. Qualitative and quantitative coronary angiography. In: Topol E, Teirstein PS. *Textbook of Interventional Cardiology, 7th edition. Elsevier; 2016*. pp 911-31.

9.Aortic Stenosis Writing Group; Bonow RO, Brown AS, Gillam LD, Kapadia SR, Kavinsky CJ, Lindman BR, Mack MJ, Thourani VH; Aortic Stenosis Rating Panel; Dehmer GJ, Bonow RO, Lindman BR, Beaver TM, Bradley SM, Carabello BA, Desai MY, George I, Green P, Holmes DR Jr, Johnston D, Leipsic J, Mick SL, Passeri JJ, Piana RN, Reichek N, Ruiz CE, Taub CC, Thomas JD, Turi ZG; Appropriate Use Criteria Task Force; Doherty JU, Dehmer GJ, Bailey SR, Bhave NM, Brown AS, Daugherty SL, Dean LS, Desai MY, Duvernoy CS, Gillam LD, Hendel RC, Kramer CM, Lindsay BD, Manning WJ, Mehrotra P, Patel MR, Sachdeva R, Wann LS, Winchester DE, Allen JM. ACC/AATS/AHA/ASE/EACTS/HVS/SCA/SCAI/SCCT/SCMR/STS 2017 Appropriate Use Criteria for the Treatment of Patients With Severe Aortic Stenosis: A Report of the American College of Cardiology Appropriate Use Criteria Task Force, American Association for Thoracic Surgery, American Heart Association, American Society of Echocardiography, European Association for Cardio-Thoracic Surgery, Heart Valve Society, Society of Cardiovascular Anesthesiologists, Society for Cardiovascular Angiography and Interventions, Society of Cardiovascular Computed Tomography, Society for Cardiovascular Magnetic Resonance, and Society of Thoracic Surgeons. *J Am Soc Echocardiogr.* 2018;31:117-47.

10. Ino Y, Toyoda Y, Tanaka A, Ishii S, Kusuyama Y, Kubo T, Takarada S, Kitabata H, Tanimoto T, Mizukoshi M, Imanishi T, Akasaka T. Predictors and prognosis of stent fracture after sirolimus-eluting stent implantation. *Circ J.* 2009;73:2036-41.

11. Nasu K, Oikawa Y, Habara M, Shirai S, Abe H, Kadotani M, Gotoh R, Hozawa H, Ota H, Suzuki T, Shibata Y, Tanabe M, Nakagawa Y, Serikawa T, Nagasaka S, Takeuchi Y, Fujimoto Y, Tamura H, Kobori Y, Yajima J, Aizawa T, Suzuki T; NO-RECOIL Registries Investigators. Efficacy of biolimus A9-eluting stent for treatment of right coronary ostial lesion with intravascular ultrasound guidance: a multicenter registry. *Cardiovasc Interv Ther.* 2018;33:321-7.

12. Fujimura T, Matsumura M, Witzenbichler B, Metzger DC, Rinaldi MJ, Duffy PL, Weisz G, Stuckey TD, Ali ZA, Zhou Z, Mintz GS, Stone GW, Maehara A. Stent Expansion Indexes to Predict Clinical Outcomes: An IVUS Substudy From ADAPT-DES. *JACC Cardiovasc Interv.* 2021;14:1639-50.

13. Lee CW, Kang SJ, Park DW Lee SH, Kim YH, Kim JJ, Park SW, Mintz GS, Park SJ. Intravascular ultrasound findings in patients with very late stent thrombosis after either drug-eluting or bare-metal stent implantation. *J Am Coll Cardiol.* 2010;55:1936-42.

14. Nakamura N, Torii S, Tsuchiya H, Nakano A, Oikawa Y, Yajima J, Nakamura S, Nakano M, Masuda N, Ohta H, Yumoto K, Natsumeda M, Ijichi T, Ikari Y, Nakazawa G. Formation of Calcified Nodule as a Cause of Early In-Stent Restenosis in Patients Undergoing Dialysis. *J Am Heart Assoc.* 2020;9:e016595.

15. Inaba S, Mintz GS, Yun KH, Yakushiji T, Shimizu T, Kang SJ, Genereux P, Weisz G, Rabbani LE, Moses JW, Stone GW, Maehara A. Mechanical complications of everolimus-eluting stents associated with adverse events: an intravascular ultrasound study. *EuroIntervention.* 2014;9:1301-8.

16. Boucek RJ, Takeshita R, Brady AH. Microanatomy and intramural physical forces within the coronary arteries (man). *Anat Rec*. 1965;153:233-41.

17. Jain SP, Liu MW, Dean LS, Babu R, Goods CM, Yadav JS, Al-Shaibi KF, Mathur A, Iyer SS, Parks JM, Baxley WA, Roubin GS. Comparison of balloon angioplasty versus debulking devices versus stenting in right coronary ostial lesions. *Am J Cardiol.* 1997;79:1334-8.

18. Kashiwagi M, Tanaka A, Kitabata H, Ino Y, Tsujioka H, Komukai K, Ozaki Y, Ishibashi K, Tanimoto T, Takarada S, Kubo T, Hirata K, Mizukoshi M, Imanishi T, Akasaka T. OCT-verified neointimal hyperplasia is increased at fracture site in drug-eluting stents. *JACC Cardiovasc Imaging.* 2012;5:232-3.

19. Nakazawa G, Finn AV, Vorpahl M, Ladich E, Kutys R, Balazs I, Kolodgie FD, Virmani R. Incidence and predictors of drug-eluting stent fracture in human coronary artery a pathologic analysis. *J Am Coll Cardiol.* 2009;54:1924-31.

20. Popma JJ, Dick RJ, Haudenschild CC, Topol EJ, Ellis SG. Atherectomy of right coronary ostial stenoses: initial and long-term results, technical features and histologic findings. *Am J Cardiol.* 1991;67:431-3.

21. Tsunoda T, Nakamura M, Wada M, Ito N, Kitagawa Y, Shiba M, Yajima S, Iijima R, Nakajima R, Yamamoto M, Takagi T, Yoshitama T, Anzai H, Nishida T, Yamaguchi T. Chronic stent recoil plays an important role in restenosis of the right coronary ostium. *Coron Artery Dis.* 2004;15:39-44.

22. Torii S, Sato Y, Otsuka F, Kolodgie FD, Jinnouchi H, Sakamoto A, Park J, Yahagi K, Sakakura K, Cornelissen A, Kawakami R, Mori M, Kawai K, Amoa F, Guo L, Kutyna M, Fernandez R, Romero ME, Fowler D, Finn AV, Virmani R. Eruptive Calcified Nodules as a Potential Mechanism of Acute Coronary Thrombosis and Sudden Death. *J Am Coll Cardiol.* 2021;77:1599-611.

23. Sugane H, Kataoka Y, Otsuka F, Nakaoku Y, Nishimura K, Nakano H, Murai K, Honda S, Hosoda H, Matama H, Doi T, Nakashima T, Fujino M, Nakao K, Yoneda S, Tahara Y, Asaumi Y, Noguchi T, Kawai K, Yasuda S. Cardiac outcomes in patients with acute coronary syndrome attributable to calcified nodule. *Atherosclerosis.* 2021;318:70-5.

24. Kang SJ, Cho YR, Park GM, Ahn JM, Kim WJ, Lee JY, Park DW, Lee SW, Kim YH, Lee CW, Mintz GS, Park SW, Park SJ. Intravascular ultrasound predictors for edge restenosis after newer generation drug-eluting stent implantation. *Am J Cardiol.* 2013;111:1408-14.

25. Dishmon DA, Elhaddi A, Packard K, Gupta V, Fischell TA. High incidence of inaccurate stent placement in the treatment of coronary aorto-ostial disease. *J Invasive Cardiol.* 2011;23:322-6.

26. Rubinshtein R, Ben-Dov N, Halon DA, Lavi I, Finkelstein A, Lewis BS, Jaffe R. Geographic miss with aorto-ostial coronary stent implantation: insights from high-resolution coronary computed tomography angiography. *EuroIntervention.* 2015;11:301-7.

27. Patel Y, Depta JP, Patel JS, Masrani SK, Novak E, Zajarias A, Kurz HI, Lasala JM, Bach RG, Singh J. Impact of intravascular ultrasound on the long-term clinical outcomes in the treatment of coronary ostial lesions. *Catheter Cardiovasc Interv.* 2016;87:232-40.

28. Honton B, Lipiecki J, Monsegu J, Leroy F, Benamer H, Commeau P, Motreff P, Cayla G, Banos JL, Bouchou G, Laperche C, Farah B, Rangé G, Lefèvre T, Amabile N; French Initiative Collaborators. Mid-term outcome of de novo lesions vs. in stent restenosis treated by intravascular lithotripsy procedures: Insights from the French Shock Initiative. *Int J Cardiol.* 2022;365:106-11.

29. Mitomo S, Naganuma T, Takagi K, Costopoulos C, Nakamura S, Hozawa K, Kurita N, Tahara S, Ishiguro H, Nakamura S. Comparison between Plain Old Balloon Angioplasty and Drug-Eluting Stent Implantation for the Treatment of Stent Fracture. *J Interv Cardiol.* 2015;28:365-73.

30. Kawamoto H, Ruparelia N, Latib A, Miyazaki T, Sato K, Mangieri A, Contri R, Stella S, Figini F, Chieffo A, Carlino M, Montorfano M, Colombo A. Drug-Coated Balloons Versus Second-Generation Drug-Eluting Stents for the Management of Recurrent Multimetal-Layered In-Stent Restenosis. *JACC Cardiovasc Interv.* 2015;8:1586-94.

Supplementary data

Supplementary Table 1. Procedural information of index PCI.

Supplementary Table 2. Comparison of primary causes between with versus without predilatation.

Supplementary Table 3. Angiographic findings for lesions with and without stent fracture.

Supplementary Table 4. Comparison of clinical and angiographical characteristics with versus without a new stent implantation for the treatment of in-stent restenosis due to a mechanical cause.

Supplementary Figure 1. Analysis of the angle between the proximal segment of the RCA and the ascending aorta.

Supplementary Figure 2. Representative cases of protruding CN, neoatherosclerotic CN, and CN behind the stent.

Supplementary Figure 3. Representative cases of stent fracture or deformation.

Supplementary Figure 4. Representative cases of full coverage (protruding stent), full coverage (non-protruding stent), partial coverage, or no coverage.

Supplementary Figure 5. Flowchart of exclusion and inclusion of lesions.

Supplementary Figure 6. Duration from stent implantation (years) stratified by primary cause of in-stent restenosis.

Supplementary Figure 7. Flowchart of exclusion and inclusion of lesions for angiographic hinge motion analysis at index and follow-up.

Supplementary Figure 8. A case example showing stent recoil.

The supplementary data are published online at: https://eurointervention.pcronline.com/doi/10.4244/EIJ-D-23-00107

Supplementary data

Supplementary Table 1. Procedural information of index PCI.

Variable	n = 105
Stent	
1st generation DES	27 (25.7%)
2nd generation DES	73 (69.5%)
Bare metal stent	5 (4.8%)
Duration between index PCI to follow-up	1.2 (0.6-3.2)
Atherectomy	
Rotational atherectomy	8/66 (12.1)
Scoring balloon	9/66 (13.6)

Values are n (%) or median (first, third quartile). DES denotes drug-eluting stent.

Supplementary Table 2. Comparison of primary causes between with versus without predilatation.

	Lesions without pre-dilatation (n=98)	All lesions (n=139)	p-value
Biological cause	51 (52.0)	74 (53.2)	0.89
Neointimal hyperplasia	27 (27.6)	35 (25.2)	0.76
Neoatherosclerosis	16 (16.3)	30 (21.6)	0.40
Uncovered ostium	8 (8.2)	9 (6.5)	0.62
Mechanical cause	47 (48.0)	65 (46.8)	0.89
Stent fracture	25 (25.5)	35 (25.2)	0.99
Underexpansion	10 (10.2)	15 (10.8)	0.99
Protruding calcified nodule	12 (12.2)	15 (10.8)	0.84

Values are n (%)

Supplementary Table 3. Angiographic findings for lesions with and without stent fracture.

Variable	Lesions with fracture (n=71)	Lesions without fracture (n=68)	p-value
Multi-vessel disease*	55 (77.5)	56 (82.4)	0.53
Calcification of ascending aorta	25 (35.2)	17 (25.0)	0.20
Target lesion calcification			
Moderate	24 (33.8)	19 (27.9)	0.47
Severe	16 (22.5)	18 (26.5)	0.69
Radiolucent mass	6 (8.5)	8 (11.8)	0.58
In stent restenosis pattern			0.51
Focal			
Proximal stent edge	52 (73.2)	48 (70.6)	
Multi focal	11 (15.5)	9 (13.2)	
Diffuse			
Intra-stent	2 (2.8)	6 (8.8)	
Proliferative	1 (1.4)	0	
Total occlusion	5 (7.0)	5 (7.4)	
Quantitative coronary angiography			
Lesion length (mm)	6.5 (5.4, 10.3)	7.1 (4.9, 12.4)	0.81
Reference vessel diameter (mm)	2.8 (2.6, 3.1)	2.8 (2.5, 3.1)	0.83
Minimum lumen diameter (mm)			
Pre-PCI	1.0 (0.75, 1.3)	1.2 (0.8, 1.5)	0.32
Post-PCI	2.7 (2.3, 3.0)	2.7 (2.4, 3.0)	0.49
Diameter stenosis (%)			
Pre-PCI	64.3 (50.8, 71.5)	56.7 (48.3, 71.8)	0.32
Post-PCI	13.9 (8.4, 24.8)	12.2 (7.7, 17.5)	0.35

Values are n (%) or median (first, third quartile). *defined as the presence of >50% luminal diameter stenosis in two or more major epicardial arteries. PCI denotes percutaneous coronary intervention

Supplementary Table 4. Comparison of clinical and angiographical characteristics with versus without a new stent implantation for the treatment of in-stent restenosis due to a mechanical cause.

	New stent (+) n=32	New stent (-) n=33	P value
Clinical characteristics			
Age (years)	72 (67, 80)	72 (66, 75)	0.35
Women	15 (46.9)	13 (39.4)	0.62
Hypertension	32 (100)	33 (100)	-
Dyslipidemia	32 (100)	33 (100)	-
Diabetes mellitus	17 (53.1)	17 (51.5)	0.99
Insulin-treated	5 (15.6)	5 (15.2)	0.99
Chronic kidney disease*	12 (37.5)	14 (42.4)	0.80
Dialysis	0 (0)	4 (12.1)	0.11
Peripheral artery disease	6 (18.8)	5 (15.2)	0.75
Prior myocardial infarction	6 (18.8)	9 (27.3)	0.56
Prior coronary artery bypass grafting	8 (25.0)	7 (21.2)	0.77
Prior or current moderate or severe aortic stenosis	5 (15.6)	4 (12.1)	0.73
Duration from prior stent implantation (years)	0.8 (0.3,2.0)	1.9 (0.7, 3.4)	0.17
Clinical presentation at the time of ISR			
Non-ST elevation myocardial infarction	3 (9.4)	4 (12.1)	0.99
Unstable angina	8 (25.0)	21 (63.6)	0.003
Stable coronary artery disease	21 (65.6)	8 (24.2)	0.001
Angiographical characteristics			
Multi-vessel disease	27 (84.4)	26 (78.8)	0.75
Calcification of ascending aorta	9 (28.1)	13 (39.4)	0.43
Target lesion calcification			
Moderate	10 (31.3)	12 (36.4)	0.79
Severe	10 (31.3)	9 (27.3)	0.79
Radiolucent mass	3 (9.4)	7 (21.2)	0.30
In stent restenosis pattern			
Focal	27 (84.4)	32 (96.8)	0.10
Proximal stent edge	24 (75.0)	28 (84.9)	0.37

Multi focal	3 (9.4)	4 (12.1)	0.99
Diffuse	2 (6.3)	1 (3.0)	0.61
Proliferative	0 (0)	0 (0)	-
Total occlusion	3 (9.4)	0 (0)	0.11
Lesion length (mm)	6.4 (5.3, 8.9)	6.3 (5.1, 9.4)	0.95
Reference vessel diameter (mm)	2.8 (2.6, 3.0)	2.8 (2.4, 3.2)	0.76
Minimum lumen diameter (mm)			
Pre-PCI	1.0 (0.8, 1.3)	1.1 (0.7, 1.5)	0.40
Post-PCI	2.7 (2.4, 3.0)	2.3 (2.2, 2.6)	0.01
Diameter stenosis (%)			
Pre-PCI	64.3 (51.4, 71.3)	60.3 (50.2)	0.45
Post-PCI	11.3 (8.2, 20.4)	21.0 (10.0, 30.3)	0.03

Values are n (%) or median (first, third quartile). *Defined as estimated glomerular filtration rate <60 mL/min/1.73 m^2 calculated using the Modification of Diet in Renal Disease equation. ISR denotes in-stent restenosis; PCI, percutaneous coronary intervention.

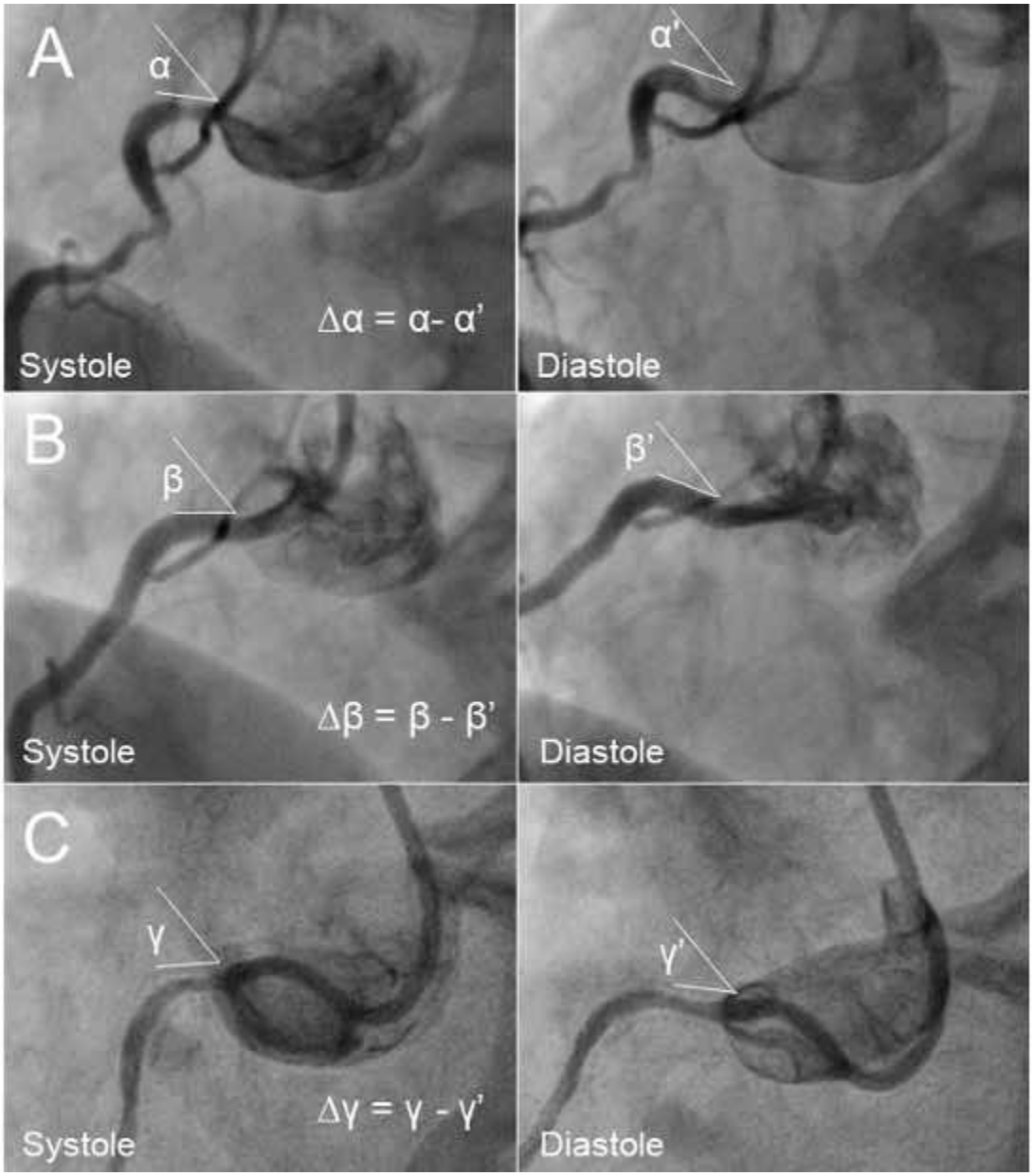

Supplementary Figure 1. Analysis of the angle between the proximal segment of the RCA and the ascending aorta.

Angle was measured during systole (α) and diastole (α') and the change (Δα = α - α') was calculated. Panel A showed pre-intervention and Panel B showed post-intervention at index procedure. Panel C showed restenosis including ostium of RCA before repeat revascularization. RCA denotes right coronary artery.

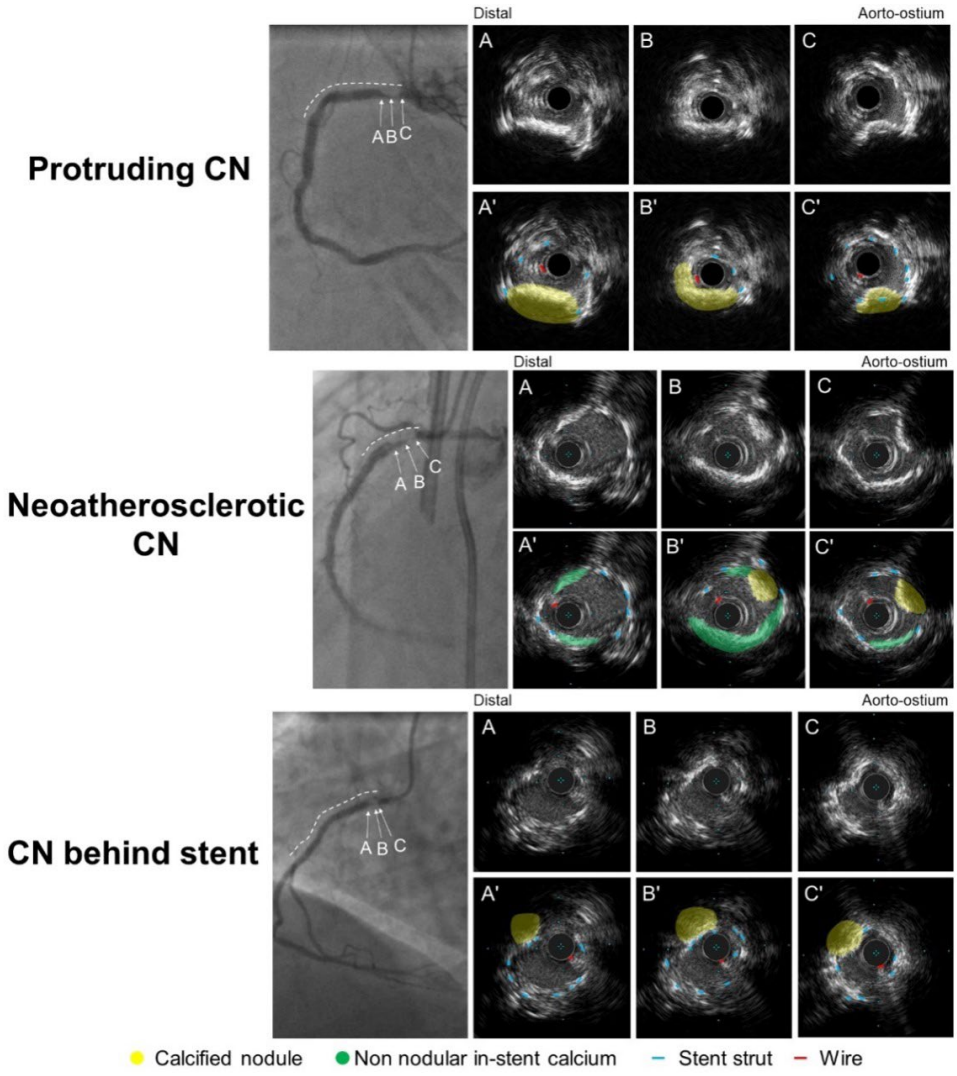

Supplementary Figure 2. Representative cases of protruding CN, neoatherosclerotic CN, and CN behind the stent.

Yellow area indicate CN and green area indicates neoatherosclerotic calcium. Top panel: There is no adjacent neointimal hyperplasia to the CN indicating protruding calcium through the stent struts. Middle panel: There is an adjacent neoatherosclerotic calcium (green area) indicating CN developed as a part of neoatherosclerosis. Bottom panel: There is a CN behind stent struts (blue dotted line) without neointimal hyperplasia or neoatherosclerosis within the stent. The

differentiation of these images requires checking proximal or distal to the current region of interest frame. CN denotes calcified nodule.

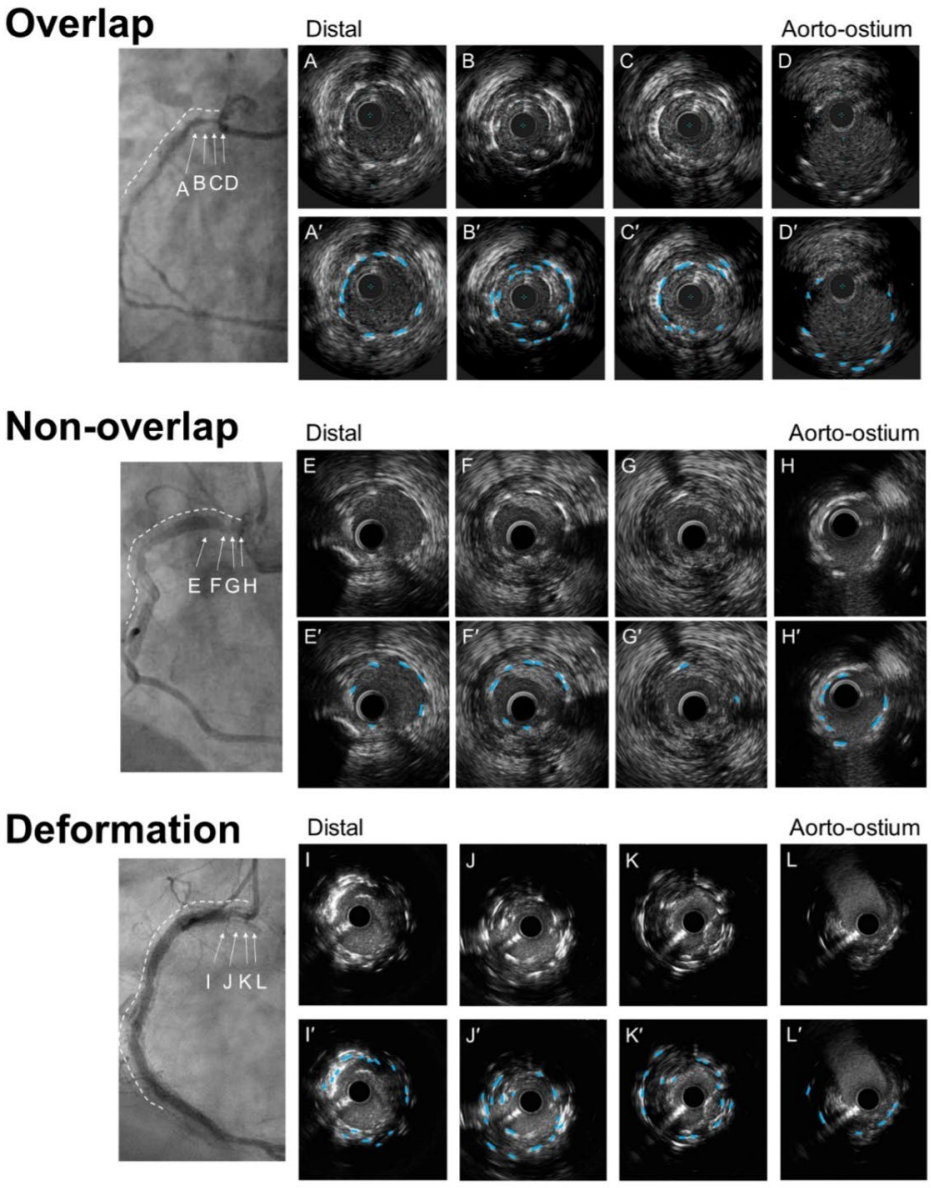

Supplementary Figure 3. Representative cases of stent fracture or deformation.

Top panel: There are double layers appearance of stent struts (blue dotted line in B and C) with preserved 3-dimentional stent integrity indicating overlapped type of stent fracture. Middle panel: There was no struts in G except one strut at 3 and 12 o'clock indicating partial stent fracture (non-overlap type). Bottom panel: There are multiple layers of stent struts with loss of 3-dimentional stent integrity indicating stent deformation.

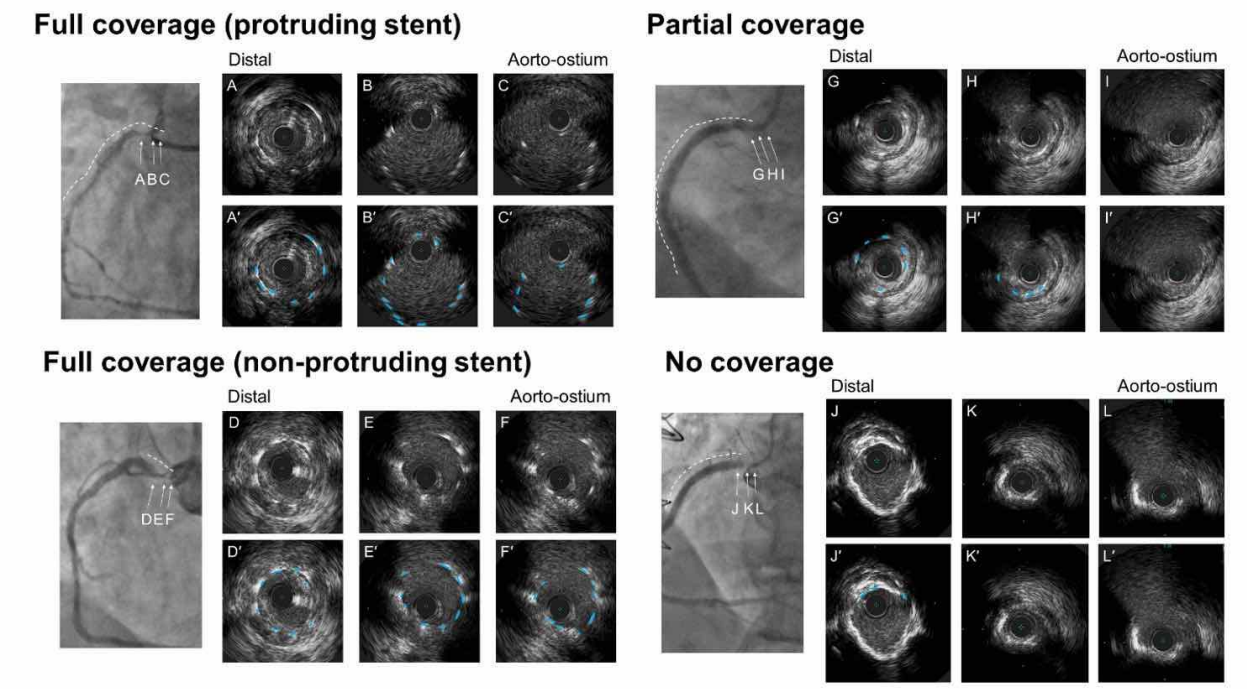

Supplementary Figure 4. Representative cases of full coverage (protruding stent), full coverage (non-protruding stent), partial coverage, or no coverage.

Top left panel: Protruding stent struts were found; thus, the ostium was fully covered. IVUS catheter was outside of stent without deforming the stent integrity (C). Bottom left panel: The

length of protruding struts measured <1mm in length. Top right panel: There is no struts at 9 to 4 o'clock (H) at the ostium indicating partial coverage of ostium. Bottom right panel: There is no strut at all at the ostium indicating no coverage of ostium (K). IVUS denotes intravascular ultrasound.

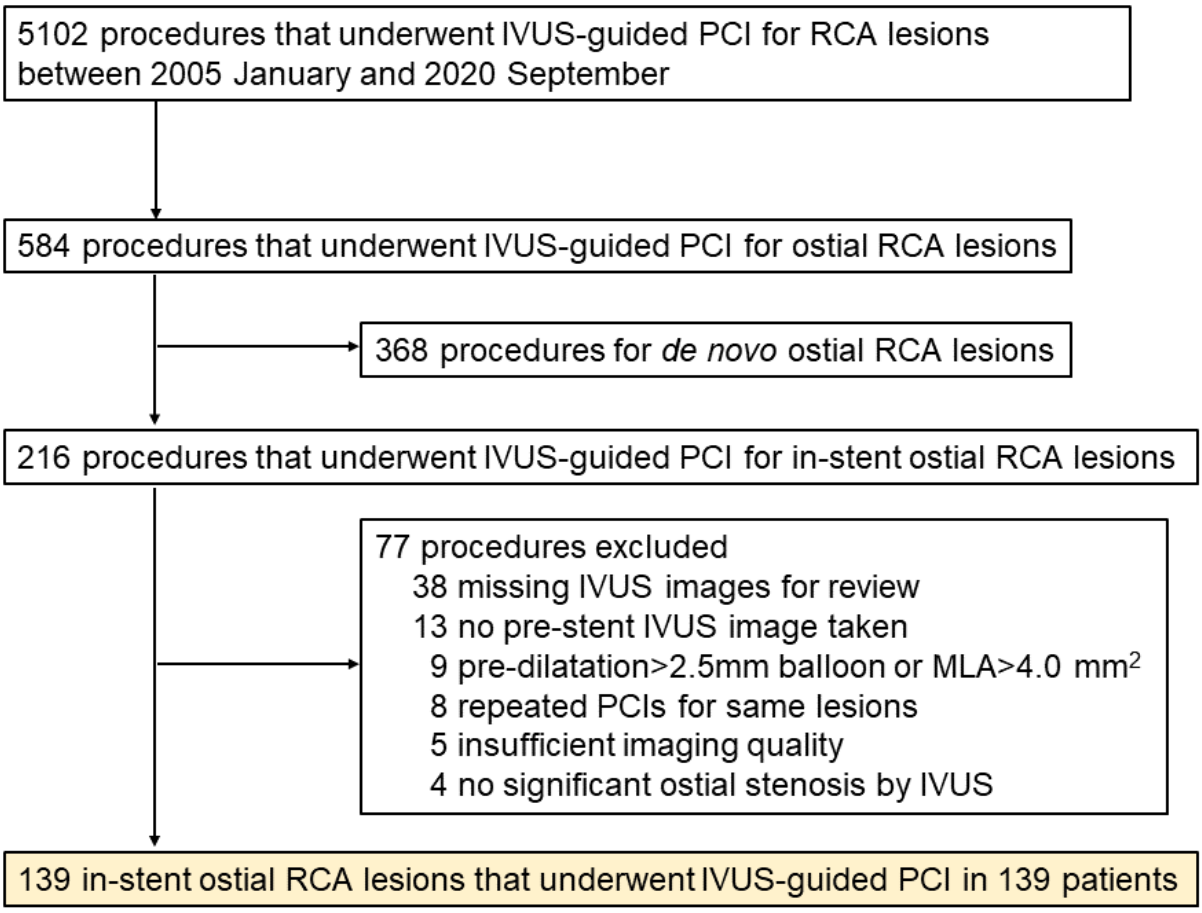

Supplementary Figure 5. Flowchart of exclusion and inclusion of lesions.

Among 5102 procedures that underwent IVUS-guided PCI for RCA lesions, finally 139 RCA ostial in-stent restenotic lesions consist of current cohort. PCI denotes percutaneous coronary intervention.

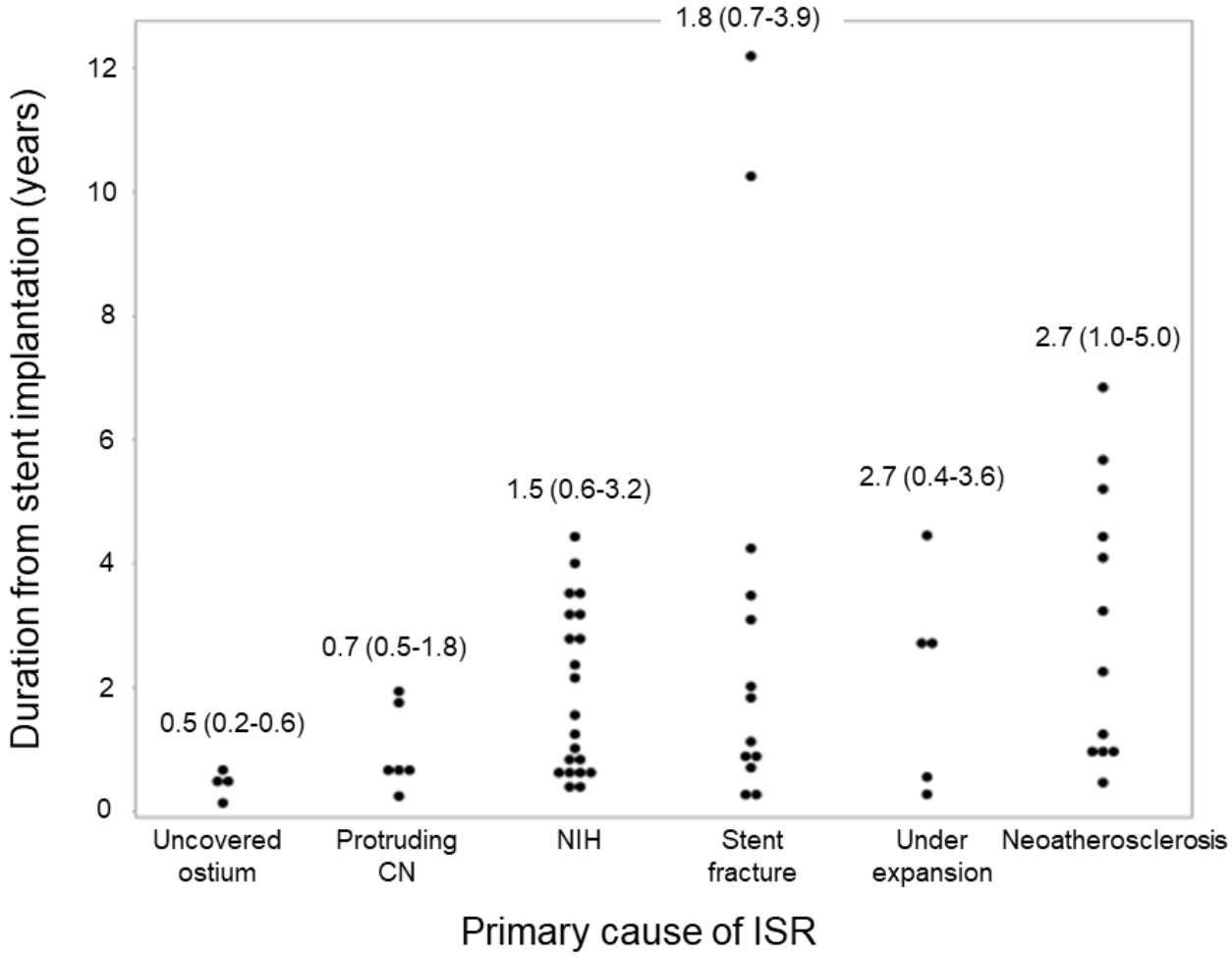

Supplementary Figure 6. Duration from stent implantation (years) stratified by primary cause of in-stent restenosis.

Except ISR lesions with stent fracture which had substantial range of duration, the other ISR occurred at different timing based on the different cause of ISRs. ISR denotes in-stent restenosis.

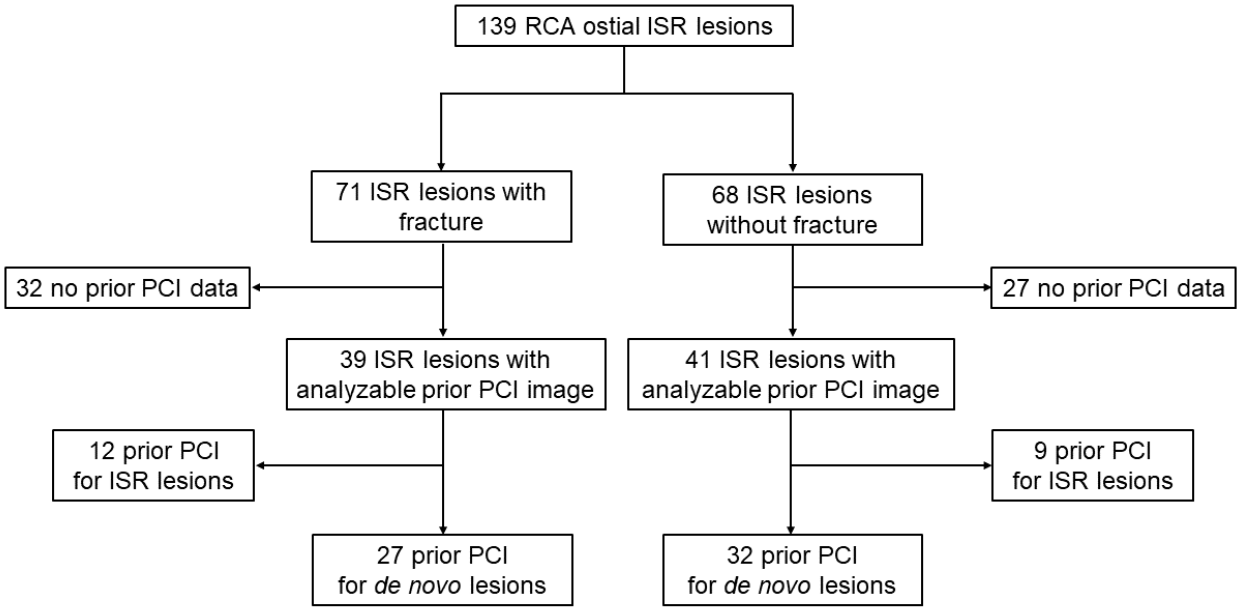

Supplementary Figure 7. Flowchart of exclusion and inclusion of lesions for angiographic hinge motion analysis at index and follow-up.

Among 139 RCA ostial ISRs, index angiography was available in 57 RCA ostial ISRs.

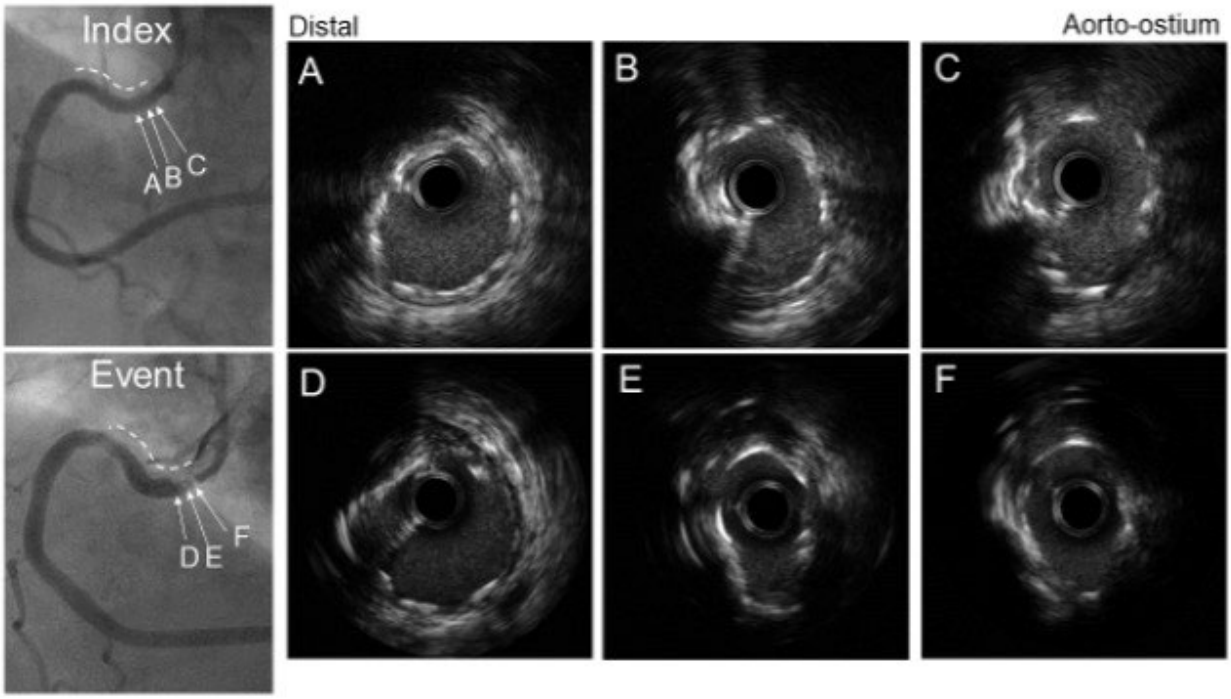

Supplementary Figure 8. A case example showing stent recoil.

The top panel showed final IVUS images at index procedure and the bottom panel showed IVUS images at the time of in-stent restenosis. Minimum stent area measured 6.4 mm^2 (B) and 5.4 mm^2 (E) indicating stent recoil, respectively.